
The Illusion of Human AI Parity Under Uncertainty: Navigating Elusive Ground Truth via a Probabilistic Paradigm

Aparna Elangovan
Independent Researcher

Lei Xu
Independent Researcher

Mahsa Elyasi *
Amazon

Ismail Akdulum †
Gazi University

Mehmet Aksakal †
University of Colorado

Enes Gurun †
Samsun University

Brian Hur
The University Of Melbourne

Saab Mansour *
Amazon

Ravid Shwartz Ziv
New York University

Karin Verspoor
RMIT University

Dan Roth
University of Pennsylvania

Abstract

Benchmarking the relative capabilities of AI systems, including Large Language Models (LLMs) and Vision Models, typically ignores the impact of uncertainty in the underlying ground truth answers from experts. This ambiguity is not just limited to human preferences, but is also consequential even in safety critical domains such as medicine where uncertainty is pervasive. In this paper, we introduce a probabilistic paradigm to theoretically explain how *high certainty in ground truth answers is almost always necessary for even an expert to achieve high scores*, whereas in datasets with high variation in ground truth answers *there may be little difference between a random labeller and an expert*. Therefore, ignoring uncertainty in ground truth evaluation data can result in the misleading conclusion that a non-expert has similar performance to that of an expert. Using the probabilistic paradigm, we thus bring forth the concepts of *expected accuracy* and *expected F1* to estimate the score an expert human or system can achieve given ground truth answer variability.

Our work leads to the recommendation that when establishing the capability of a system, results should be stratified by probability of the ground truth answer, typically measured by the agreement rate of ground truth experts. Stratification becomes critical when the overall performance drops below a threshold of 80%. Under stratified evaluation, performance comparison becomes more reliable in high certainty bins, mitigating the effect of the key confounding factor — uncertainty.

1 Introduction

Artificial Intelligence (AI) systems, including large language models (LLMs), are typically evaluated against ground truth (GT) human labels under the simplistic assumption that a single correct or a

*Work done outside Amazon

†Equal Contributions

preferred answer can be associated with a test question. Conventional evaluation simply compares the performance of an AI model or algorithm against that of a doctor to benchmark the relative capabilities of the model, ignoring the impact of uncertainty in the underlying ground truth labels. In this paper, through a probabilistic paradigm, we demonstrate why datasets that have variation in ground truth answers show two characteristics: **(a)** high certainty in ground truth answers is almost always necessary for an expert to achieve high scores on an evaluation set, as measured by typical ground truth uncertainty agnostic metrics such as accuracy or F1 scores, and **(b)** when certainty in ground truth answers is low (or equivalently, uncertainty is high), there may not be any difference between a random labeller and an expert.

Humans can rely on heuristics or mental shortcuts to make decisions which are often noisy under uncertainty [22, 21]. Uncertainty plays a vital role safety critical applications such as in medicine, where uncertainty remain a hidden component in the diagnosis, treatment, and prognosis of disease [27, 14, 23, 15, 13, 11, 4]. In diagnostic decision making, this uncertainty has often been likened to searching for a “*snowball in a blizzard*” [16]. Yet, when comparing AI models to doctors, uncertainty is often ignored. Medical uncertainty can be the result of many factors, ranging from incomplete scientific data for certain conditions, lack of comprehensive information about a patient, complexity of clinical information, the probabilistic nature of certain outcomes, practical constraints such as time and cost [23, 17, 4] and cognitive biases [32]. As an example, when patients present with undifferentiated symptoms it is difficult for clinicians to identify a satisfactory explanation of the patient’s problem, especially under finite pragmatic constraints such as time and cost [17]. Despite the role of uncertainty in medicine, popular data sets such as MedQA [19] have a single definitive answer associated with each question in the dataset, which are then used to evaluate LLMs [33]. Such datasets rarely capture the medical ambiguity encountered in practice. Recent works have begun to investigate the impact of human label uncertainty on model training and evaluation [29, 10, 28], including the illusion that LLM-as-a-judge approximating human majority may be an artifact of high uncertainty in ground truth human labels [10]. Stutz et al. [35] also show that ignoring uncertainty leads to overly optimistic estimates of model performance for a dermatology dataset.

Our contribution in this paper is to provide a probabilistic model, to estimate the impact of uncertainty on evaluation. We measure certainty through considering agreement on ground truth labels between multiple experts — with high agreement implying high *certainty*, and lower agreement corresponding to *uncertainty* in the data. When only one annotation is collected per item, the associated uncertainty is simply not quantified.

Our probabilistic model supports the empirical results to demonstrate the following two arguments:

1. Wherever ground truth tends to be subjective, including domains like medicine, *high certainty in ground truth is almost always necessary, but not sufficient, for human experts and models to achieve high performance* as measured by ground truth uncertainty agnostic metrics such as F1 or accuracy. Here, the ground truth correct answer is implicitly or explicitly based on a majority label and is not objective.
2. *High uncertainty in ground truth answers cannot effectively disambiguate between a weak and strong performer*. Hence, when the uncertainty is high or simply not quantified, it can lead to the incorrect conclusion that a weak and a strong performer have similar capabilities. As an example, if two expert doctors disagree on the presence of a certain disease, even an answer selected by a random coin flip cannot be wrong, as its answer will match one of the two experts and its performance will be similar to one of the doctors.

We also demonstrate this empirically using the popular CheXpert [18] dataset which consists of chest radiographs of patients from Stanford Health Care between 2002 and 2017, where each X-ray in the evaluation set (500 X-rays) is annotated by 5 radiologists providing ground truth, and the performance of 3 additional human radiologists is also captured, allowing us to systematically measure and capture human ambiguity and compare human experts as well as model performance with ground truth. We also analyse an existing published dataset, with over 200,000 samples, from AI mammogram screening results deployed nationwide in Germany [7].

2 Theory – A probabilistic paradigm for uncertainty and its impact on metrics

In order to explain why it is highly unlikely even for an expert to achieve over 90% performance on a dataset that has high disagreement rates among experts themselves, we present the following statistical analysis.

Let us assume that in general doctors have a probability p_d of following the consensus of other doctors on the majority label. For instance, if for a given diagnosis, 3/5 doctors indicate agreement on a finding while 2/5 disagree on that finding, here $p_d = \frac{3}{5} = 0.6$ on the majority finding. When p_d is computed empirically from the dataset by counting how many votes the majority answer gets compared to the total number of answers for that item, it is the observed p_d . The observed p_d tends to be a closer approximation to true underlying p_d as more opinions or answers are collected per item. When only one answer or opinion is collected per item, it does *not* imply that p_d is 1.0 (1/1), but rather that the underlying p_d simply cannot be computed empirically. In the case of a consensus answer determined by an independent adjudicator when 2 doctors disagree, the p_d on the adjudicator’s label is not 1.0, since the majority label may change when the adjudicator changes. That is, we should treat the adjudicator’s label as simply another experts’s opinion. In the remainder of the paper, we assume that the observed p_d is a close enough approximation of the true underlying p_d .

We make the following 3 assumptions:

1. The ground truth answer against which any automatic system or another expert is compared to is a *majority label*. This is typically the case for subjective problems, where the ground truth is either explicitly or implicitly an assumed majority label.
2. The probability of an expert following the consensus of similarly trained peer group to select the majority label is p_d , where p_d is also the probability of agreeing with the majority label.
3. The answer that an expert selects is independent of what the other experts select (meaning that an expert is not influenced as a result of someone else’s answer).

Using the above assumptions, we can model the problem of an expert selecting the majority (correct) label as a biased coin toss problem, where the probability of a head is p_d , so the probability of obtaining heads is equivalent to selecting the majority label. Then, directly following the Binomial distribution, in a sample of N examples, the probability of getting *at least* r_c items correct ($P(\text{Score} \geq r_c)$) is

$$\text{Expected score} = E(\text{Score}) = p_d \quad (1)$$

$$P(\text{Score} \geq r_c) = 1 - \sum_{k=0}^{r_c-1} \binom{N}{k} p_d^k (1-p_d)^{(N-k)} \quad (2)$$

Applying the above equation, the probability that a doctor obtains at least 50 of 100 correct (in other words, the majority label matches), i.e., ($r_c \geq 50$), given that the probability of following the majority label $p_d = 0.6$ is 0.98. On the other hand, the probability of obtaining more than 80% correct ($r_c \geq 80$ out of 100 samples) drops to near zero $1.6e - 5$ as shown in Table 1.

On the other hand, assume that p_d is 0.9, where 9 out of 10 doctors arrive at the same conclusion, then the probability of any other doctor who follows the same distribution obtaining a score of 80% score or higher increases from near zero (when $p_d = 0.6$) to 0.99 as shown in Table 1.

Further comparing this behavior with a weak labeller, let us take a random labeller who randomly chooses to either agree or disagree with the majority label. In that case, random labeller probability is $p_r = 0.5$ while a doctor who follows majority consensus in a highly uncertain dataset $p_d = 0.5$ and then there is 50% chance that the doctor and the random labeller will achieve the same average score of 50%. On the other hand, on a dataset with $p_d = 0.9$, the average performance of a random labeller is only 50% while that of a perform that follows a typical doctor’s distribution has a 50% probability of achieving more than 90% accuracy. **Note:** As shown in Table 1, when the sample size is small (say $N = 10$), even a random labeller has a 5% chance of over 80%, compared to a chance of near zero when the sample size is 100.

p_d	$N = 100$		$N = 10$	
	r_c	$P(\text{Score} \geq r_c)$	r_c	$P(\text{Score} \geq r_c)$
$p_d = p_r = 0.5$	Random labeller baseline			
0.5	50	0.54	5	0.62
0.5	80	5.6e-10	8	0.05
0.6	50	0.98	5	0.83
0.6	80	1.6e-5	8	0.17
0.9	50	1.00	5	0.99
0.9	80	0.99	8	0.92

Table 1: Examples of how given the probability p_d of following the majority label, the corresponding probability of achieving over 50% or 80% accuracy changes out of N 100 examples vs. 10 examples. p_r is the random labeller ($p_d=0.5$).

In summary, in a dataset that contains high uncertainty where agreement on what the correct answer is near borderline (say $p_d = 0.5$ and that of random labeller $p_r = 0.5$), then there is 0.5 probability that the strong and weak labeller will achieve a score greater than or equal to 50% and therefore, may not be able to effectively differentiate between a strong and a weak performer. High agreement datasets are therefore almost always required for even an expertly trained doctor to reach high scores where the correct answer is either implicitly or explicitly the majority label. We further demonstrate this phenomena empirically in real world datasets in Section 4, where the performance of human experts generally tends to drop at $p_d = 0.6$ compared to $p_d = 1.0$.

2.1 The impact of class imbalance

Real-world datasets, especially in medicine, tend to be skewed, where there may be very few positive examples especially when the disease or condition has low prevalence. Assume that given N samples, the fraction m , where $0 < m < 1$, represents the proportion of positive samples. For example, $N = 100$, $m = 0.2$ indicates that 20 ($0.2 * 100 = 20$) examples are positive according to the majority ground truth label.

To understand how m impacts precision and recall given p_d , the probability of selecting the majority label, we estimate the expected (average) number of true positives (TP), False Positives (FP), False Negatives (FN) and True Negatives (TN) as follows:

$$E(TP) = m * N * (p_d) \quad (3)$$

$$E(FN) = m * N * (1 - p_d) \quad (4)$$

$$E(FP) = (1 - m) * N * (1 - p_d) \quad (5)$$

$$E(TN) = (1 - m) * N * (p_d) \quad (6)$$

$$E(\text{Precision}) = \frac{TP}{TP + FP} = \frac{m * p_d}{m * p_d + (1 - m)(1 - p_d)} \quad (7)$$

$$E(\text{Recall}) = \frac{TP}{TP + FN} = p_d \quad (8)$$

$$E(F1) = \frac{2 * \text{Precision} * \text{Recall}}{\text{Precision} + \text{Recall}} = \frac{2 * m * p_d}{2 * m * p_d + 1 - p_d} \quad (9)$$

$$E(\text{Accuracy}) = \frac{TP + TN}{TP + FP + TN + FN} = p_d \quad (10)$$

From the above equation, the labeller who follows the distribution p_d to select the majority label, the recall is independent of m . Precision is impacted by m or the class balance ratio as shown above. If m is very low at 0.01 (or high class imbalance which is often the case of rare diagnosis), at even high certainty datasets, say $p_d = 0.9$, the expected precision would be as low as 0.08 as shown computationally in Table 2.

An extension to the above equation is the case where in a dataset of N samples, there are k different agreement distributions, where $p_d \in p_1..p_k$, with $n_1, ..n_k$ samples where $N = \sum_k n_k$ and the

p_d (Expected Recall)	m	Expected Precision	Expected F1
$p_d = p_r = 0.5$			
Random labeller baseline			
0.5	0.01	0.01	0.02
0.5	0.10	0.10	0.17
0.5	0.50	0.50	0.50
<hr/>			
0.6	0.01	0.01	0.03
0.6	0.10	0.14	0.23
0.6	0.50	0.60	0.60
<hr/>			
0.9	0.01	0.08	0.15
0.9	0.10	0.50	0.64
0.9	0.50	0.90	0.90

Table 2: Examples showing how given probability p_d following the majority label, the positive class ratio m , the expected precision and F1 increases with increasing m .

corresponding positive clas ratio $m_1 \dots, m_k$ (note: m is wrt n_k).

$$E(\text{Precision}) = \frac{\sum_1^k n_k * m_k * p_k}{\sum_1^k n_k (m_k * p_k + (1 - p_k) * (1 - m_k))} \quad (11)$$

$$E(\text{Recall}) = \frac{\sum_1^k n_k * m_k * p_k}{\sum_1^k n_k * m_k} \quad (12)$$

$$E(\text{Accuracy}) = \frac{\sum_1^k n_k * p_k}{N} \quad (13)$$

3 Simulation

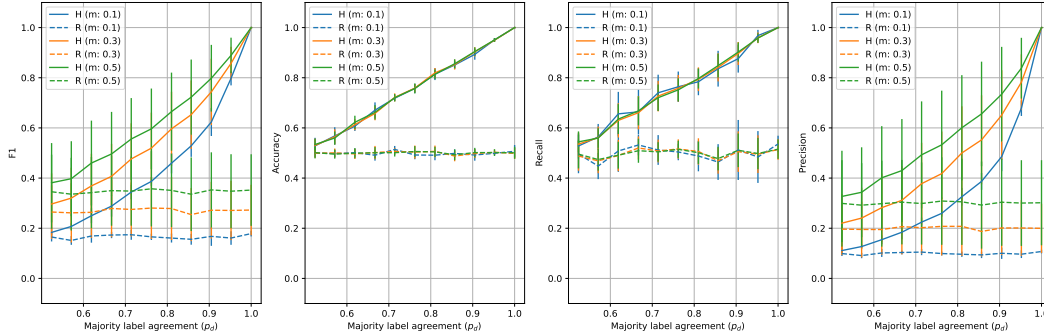


Figure 1: Simulating the impact of agreement for the majority label (X axis). The Y axis is the performance of a simulated human (**H**) who follows the majority label distribution (p_d) vs. the random labeller (**R**) performance across different positive label ratios $m \in 0.1, 0.3, 0.5$. At low certainty, the difference between human labeller distribution and random labeller is relatively low compared to high certainty. Recall and Accuracy are unaffected by the positive label ratio. The vertical bars indicate standard deviation.

We also simulate the behavior of a random labeller (who randomly picks one of the 2 binary labels with $\frac{1}{2}$ probability) vs. an expert (who tends to follow the rest of the experts' label distribution) using synthetically generated labels. Say, when a group of experts have $\frac{3}{5}$ probability of selecting the same label, then another expert is likely to also have the same chance ($\frac{3}{5}$) of selecting the same label. We also include varying positive sample ratios in the simulation as shown in Figure 1. The difference between the random labeller and the simulated human narrows during high uncertainty as shown in Figure 1. In addition, simulated human performance drops even lower, in addition to p_d , when the positive class ratio is low.

4 Empirical Results

We compare the performance of the state-of-the-art (SOTA) multimodal-LLMs, Gemini-3-Preview, GPT 5.1 and GPT 2.5 pro to human radiologists for the CheXpert dataset [18]. Each X-ray in the CheXpert dataset has 12 pathologies (e.g. Atelectasis, Cardiomegaly, and Edema) annotated by 5 ground truth radiologists independently. Each pathology is treated as a binary classification problem (positive finding, no finding). The extent of uncertainty in ground truth is shown in Appendix Figure 4, where samples with high agreement on positive findings drop substantially to less than 1% .

Given the extent of uncertainty in ground truth labels, in addition to a typical aggregate results that does *not* account for uncertainty, we also stratify the results by the probability (p_d) of agreement among experts for the majority label, where p_d is computed empirically from the dataset. As an example, say out of the 5 ground truth set of experts, 4 have selected the same label to form the majority, then $p_d = \frac{4}{5} = 0.8$. As shown in Figure 2, there are 3 key observations related to absolute performance that experts can achieve at high p_d and as p_d drops the relative *lack of difference* to a non-expert.

1. As $p_d \rightarrow 1.0$, the average human F1 across pathologies with $m \geq 0.1$ is 0.89 ± 0.1 , while the F1 including the 4 pathologies that have $m < 0.1$ is 0.71 ± 0.27 . As $p_d \rightarrow 1.0$, the average accuracy (independent of m) is $0.95 \pm .02$ and the expected accuracy $\rightarrow 1.0$ according to Equation 1. In pathologies where the models do perform well, the peak performance is also as $p_d \rightarrow 1.0$, with Gemini 3 and GPT 5 scoring an F1 0.89 and 0.90 respectively for Lung Opacity as shown in Table 3. In short, this absolute high performance, regardless of model or human, occurs in bins with high ground truth agreement as $p_d \rightarrow 1.0$.
2. As a consequence, when the agreement between ground truth radiologists is high, some of the largest performance gap can be observed between human radiologists and models in pathologies *where models do not perform particularly well*. For instance, for Support Devices, humans achieve F1 0.98 ($p_d \rightarrow 1.0$), and the $\Delta = H - M$ compared to models is over 22 points for both Gemini 3 and GPT 5.1 as shown in Table 3.
3. As a corollary, the performance of humans drops substantially at low agreement ($p_d \rightarrow 0.6$) with an average F1 of $0.55 \pm .15$, accuracy $0.63 \pm .02$ and expected accuracy of 0.6 according to Equation 1. Here, the relative performance difference narrows down the most between the human radiologists and models *even in pathologies where models do not perform particularly well*, with models outperforming the radiologists in some cases. For instance, for Support Devices, human performance drops from F1 0.98 ($p_d \rightarrow 1.0$) to F1 0.72 ($p_d \rightarrow 0.6$), whereas the performance of all 3 models remains largely the same 0.76 ± 0.02 , outperforming radiologists by 4 ± 2 points. *Notes on sample size:* At $p_d \rightarrow 0.6$ with very few samples ($N \leq 12$), humans can achieve an accuracy of 0.8 (see Appendix Table 7), and this statistically has a $\approx 22\%$ chance at $N = 12$ according to Equation 2 compared to near zero with a sample size of 100.

The overall distribution of $\Delta = H - M$, where Δ tends to be relatively higher $p_d \rightarrow 1.0$ compared to $p_d \rightarrow 0.6$ where average $\Delta = H - M$ for F1 drops to near zero, is further illustrated in Figure 3. Without stratification by uncertainty, based on aggregate performance, we would have drawn a misleading conclusion that there is no statistically significant difference between a weak algorithm (including models) and expert doctors. For instance, previous studies have reported [37, 26] that the models achieve expert level performance in CheXpert dataset, where the model scores F1 0.60 while the radiologists score F1 0.62 across 5 pathologies. Drawing parallels to our study, for instance for Cardiomegaly, the difference between human and Gemini 3 $\Delta = 0.68 - 0.66 = 0.02$, but as $p_d \rightarrow 1.0$ the performance of the Gemini 3 model compared to humans is much lower with $\Delta = 0.35$ as shown in Table 3.

In the population-wide mammogram screening dataset [7], which has public results for their proprietary AI model, we reuse existing results and stratify them by p_d . In this dataset, 2 doctors independently provide their finding and when there is disagreement, a third consensus label is used as the ground truth. We select the set of around 200000 samples where doctors provided their finding (normal, suspicious) without AI assistance, and compare the doctors' majority finding with the model's prediction. Since in this dataset another independent doctor's finding label is not available to compare with the ground truth, we randomly select one of the labels 5 times from the ground truth labels and average the score to mimic the performance of another human H' . As shown in Table 4,

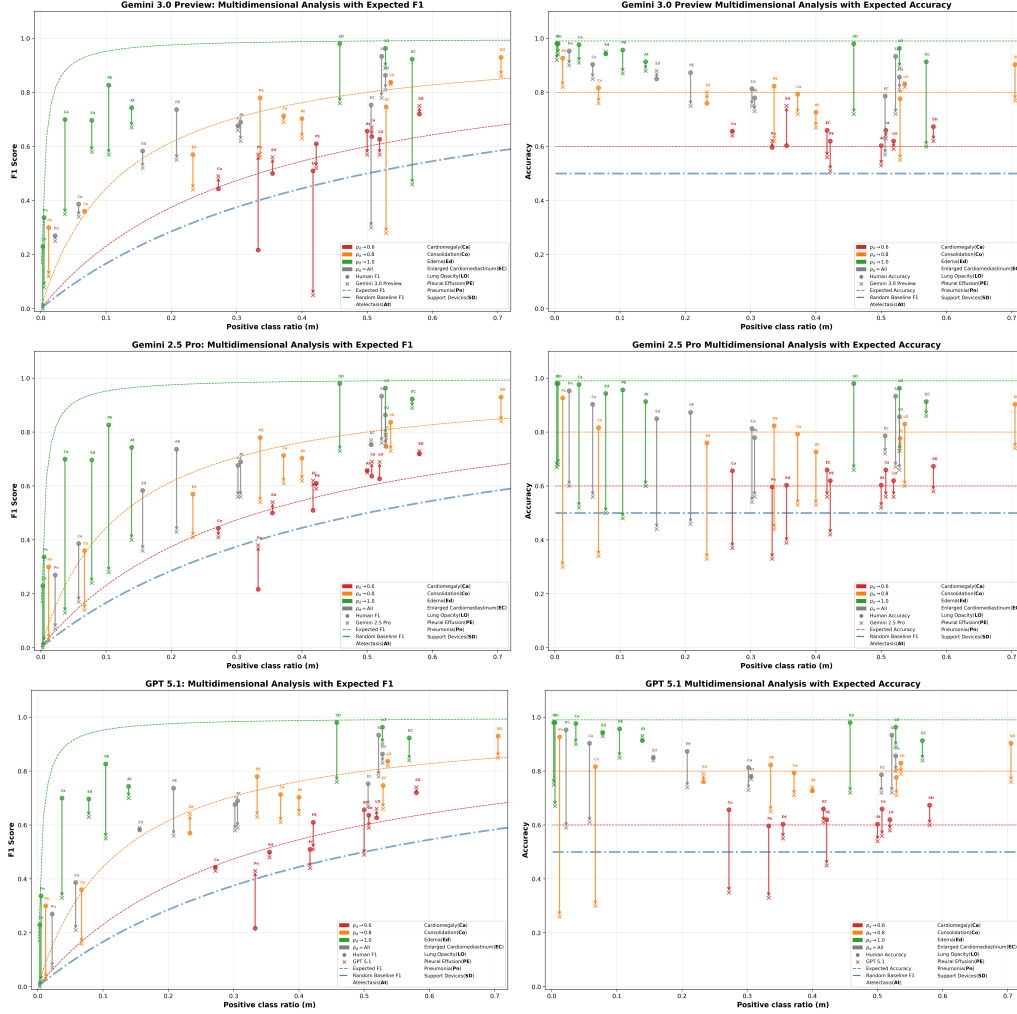


Figure 2: Performance of Models (**M**) vs. human (**H**) radiologists, compared against ground truth (majority label across 5 human radiologists). **H** is the average performance of additional 3 radiologists who are different from the 5 radiologists used to determine the ground truth. The data is stratified by p_d probability of observed agreement among the 5 radiologists for the majority label, corresponding positive class ratio is m . Dashed lines are theoretical expected performance at given p_d and m according to equations 1 and 9, ($p_d \rightarrow 1.0$ is approximated as $p_d = 0.985$). Humans are able to achieve a relatively high F1-score (> 0.8) as $p_d \rightarrow 1.0$, whereas $p_d \rightarrow 0.6$ the peak performance drops close to a random labeller baseline. At low positive class ratio ($m < 0.01$), even at $p_d \rightarrow 1.0$ (see Pneumonia and Consolidation), F1 is < 0.35 . $\Delta = H - M$ is the vertical distance illustrated by the length of the vertical line connecting the human and the model performance. For Pneumonia, humans have much lower than expected F1 as $p_d \rightarrow 0.6$, but it has only 22 samples in that bin. Detailed tabular data is in Appendix Tables 6, 7, and 8.

H' drops dramatically to 0.48 F1 (expected F1 is 0.48 as per Equation 9), while accuracy is 0.67 (expected accuracy is 0.67 Equation 1), and as a consequence the Δ between humans and the model narrows down the most.

5 Discussion

The role of ground truth uncertainty and the performance of automated systems (such as LLMs or AI any system) is a subject of recent investigations uncovering a plethora of challenges [10, 36, 24, 3]. These include the impact of ignoring ground truth uncertainty [10, 29, 39, 35] to the applicability

GT annotation size = 5				F1			Precision			Recall			Accuracy		
Pathology	p_d	S	m	M	H	Δ	M	H	Δ	M	H	Δ	M	H	Δ
Gemini 3.0 Preview															
Lung Opacity	0.6	106	0.519	0.57	0.63±0.07	0.06	0.63	0.64±0.01	0.01	0.53	0.62±0.13	0.09	0.59	0.62±0.03	0.03
	0.8	125	0.536	0.83	0.84±0.03	0.01	0.83	0.87±0.05	0.04	0.82	0.82±0.06	-0.00	0.82	0.83±0.03	0.01
	1.0	269	0.528	0.89	0.96±0.01	0.07	0.95	0.95±0.02	-0.00	0.84	0.98±0.02	0.14	0.89	0.96±0.01	0.07
	All	500	0.528	0.81	0.86±0.02	0.05	0.86	0.87±0.03	0.01	0.77	0.86±0.05	0.09	0.81	0.86±0.01	0.05
Cardio-megaly	0.6	142	0.507	0.67	0.64±0.10	-0.03	0.61	0.71±0.09	0.10	0.75	0.62±0.22	-0.13	0.63	0.66±0.03	0.03
	0.8	196	0.372	0.69	0.71±0.04	0.02	0.59	0.74±0.11	0.15	0.82	0.72±0.15	-0.10	0.72	0.79±0.03	0.07
	1.0	162	0.037	0.35	0.70±0.12	0.35	0.24	0.69±0.17	0.45	0.67	0.78±0.25	0.11	0.91	0.98±0.02	0.07
	All	500	0.302	0.66	0.68±0.07	0.02	0.57	0.72±0.11	0.15	0.78	0.68±0.19	-0.10	0.75	0.81±0.03	0.06
Support Devices	0.6	50	0.580	0.75	0.72±0.04	-0.03	0.60	0.75±0.12	0.15	1.00	0.74±0.20	-0.26	0.62	0.67±0.05	0.05
	0.8	105	0.705	0.86	0.93±0.02	0.07	0.77	0.95±0.04	0.18	0.96	0.92±0.06	-0.04	0.77	0.90±0.02	0.13
	1.0	345	0.458	0.76	0.98±0.00	0.22	0.62	0.99±0.02	0.37	0.96	0.97±0.02	0.01	0.72	0.98±0.00	0.26
	All	500	0.522	0.78	0.93±0.01	0.15	0.66	0.95±0.05	0.29	0.97	0.93±0.05	-0.04	0.72	0.93±0.01	0.21
GPT 5.1															
Lung Opacity	0.6	106	0.519	0.66	0.63±0.07	-0.03	0.56	0.64±0.01	0.08	0.80	0.62±0.13	-0.18	0.58	0.62±0.03	0.04
	0.8	125	0.536	0.82	0.84±0.03	0.02	0.75	0.87±0.05	0.12	0.91	0.82±0.06	-0.09	0.79	0.83±0.03	0.04
	1.0	269	0.528	0.90	0.96±0.01	0.06	0.86	0.95±0.02	0.09	0.95	0.98±0.02	0.03	0.89	0.96±0.01	0.07
	All	500	0.528	0.83	0.86±0.02	0.03	0.76	0.87±0.03	0.11	0.91	0.86±0.05	-0.05	0.80	0.86±0.01	0.06
Cardio-megaly	0.6	142	0.507	0.59	0.64±0.10	0.05	0.56	0.71±0.09	0.15	0.61	0.62±0.22	0.01	0.56	0.66±0.03	0.10
	0.8	196	0.372	0.61	0.71±0.04	0.10	0.62	0.74±0.11	0.12	0.60	0.72±0.15	0.12	0.71	0.79±0.03	0.08
	1.0	162	0.037	0.33	0.70±0.12	0.37	0.22	0.69±0.17	0.47	0.67	0.78±0.25	0.11	0.90	0.98±0.02	0.08
	All	500	0.302	0.58	0.68±0.07	0.10	0.55	0.72±0.11	0.17	0.61	0.68±0.19	0.07	0.73	0.81±0.03	0.08
Support Devices	0.6	50	0.580	0.74	0.72±0.04	-0.02	0.59	0.75±0.12	0.16	1.00	0.74±0.20	-0.26	0.60	0.67±0.05	0.07
	0.8	105	0.705	0.85	0.93±0.02	0.08	0.76	0.95±0.04	0.19	0.96	0.92±0.06	-0.04	0.76	0.90±0.02	0.14
	1.0	345	0.458	0.76	0.98±0.00	0.22	0.63	0.99±0.02	0.36	0.96	0.97±0.02	0.01	0.72	0.98±0.00	0.26
	All	500	0.522	0.78	0.93±0.01	0.15	0.66	0.95±0.05	0.29	0.96	0.93±0.05	-0.03	0.72	0.93±0.01	0.21

Table 3: Detailed examples of models (M) Gemini 3 and GPT 5.1 performance variation when stratified by p_d compared to average human (H) performance of 3 radiologists and the corresponding standard deviation, sample size S. For Lung Opacity, the overall ($p_d = All$) performance is over 80%, and even at stratified p_d , the models achieves reasonable F1 and accuracy scores compared to humans. On the other hand, for Cardiomegaly and Support Devices the overall ($p_d = All$) performance falls below 80% and Gemini even achieves a $\Delta = H - M$ of just 2 points for Cardiomegaly, however as $p_d \rightarrow 1$, the Δ is over 20 points. Full results are in Appendix Tables 6, and 8.

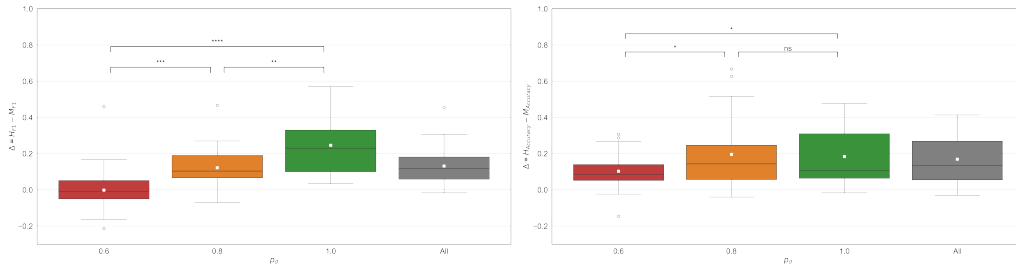


Figure 3: Distribution of $\Delta = H - M$ in scores using a boxplot across all 3 models, where each $\Delta_{i,o,p_d} = H_{o,p_d} - M_{i,o,p_d}$ where $i \in \{\text{Gemini 3, Gemini 2.5, GPT 5.1}\}$, $p_d \in \{0.6, 0.8, 1.0, All\}$, $o \in \text{Pathologies}$. H_{o,p_d} is the human score (F1 or accuracy) against the pathology o at p_d . Similarly, M_{i,o,p_d} is the performance of the model i against the pathology o at p_d . Average Δ is generally higher as $p_d \rightarrow 1.0$ compared to $p_d \rightarrow 0.6$ where Δ F1 is close to zero. Significance t-test: **** ($p <= 0.0001$), *** ($p <= 0.001$), ** ($p <= 0.01$), * ($p <= 0.05$), ns (not significant).

GT size = (2, 3)			F1						Accuracy (A)					
p_d	S	m	AI	H'	E	$\Delta_{H'-AI}$	$\Delta_{E-H'}$	Δ_{E-M}	AI	H'	E	$\Delta_{H'-AI}$	$\Delta_{E-H'}$	Δ_{E-M}
0.67	15834	0.229	0.39	0.48±0.0045	0.48	0.09	0.00	0.09	0.42	0.67±0.0045	0.67	0.25	0.00	0.25
1.00	185245	0.029	0.11	1.00±0.0000	1.00	0.89	-0.00	0.89	0.58	1.00±0.0000	1.00	0.42	0.00	0.42
ALL	201079	0.045	0.15	0.75±0.0000	0.75	0.60	-0.00	0.60	0.56	0.97±0.0000	0.97	0.41	0.00	0.41

Table 4: Stratified performance on existing results on Mammogram from Eisemann et. al. [7]. S is the sample size, $F1\Delta = H' - AI$ drops dramatically as $p_d \rightarrow 0.67$ to 0.09, as human performance drops to 0.48 F1.

(or inapplicability) and interpretation (or misinterpretations) of typical inter-rater agreement (IRA) metrics such as Cohen’s- κ [5], Krippendorff’s- α [25] and Spearman’s ρ correlation. Fundamentally, IRA metrics are designed for when no ground truth is available [25] and make assumptions about human behavior under cognitive uncertainty to account for chance agreement [41, 30, 25]. For instance, when humans rate based on a 1-5 Likert scale, choosing an in-between rating of 3 (neutral) tends to be a result of uncertainty [2] and hence high agreement when the rating is 3 may not be particularly useful and hence metrics such as Krippendorff’s- α penalize low agreement on minority labels compared to high frequency labels [25]. IRA scores are quite difficult to visualize to meaningfully interpret and critically review the gaps in the metric adding to the confusion, with recent works proposing the use of perception charts [10] to alleviate some of these challenges. IRA metrics further assume that high agreement is good and low agreement is not, and ignore the fact that some tasks are just fundamentally ambiguous. At the very core, any aggregate metric is only as reliable as its ability to effectively summarize the underlying data [12] and any gaps in the metric may be difficult to identify without detailed analysis. In summary, there are clear gaps in existing metrics as shown in Table 4 and 3, with respect to their ability to deal with ground truth uncertainty where the detailed analysis presents a very different conclusion compared to the one depicted by the aggregate metric.

Another question is whether low agreement limits machine learning performance and in this paper we probabilistically show how when certainty is low quantified by p_d , say when $p_d \rightarrow 0.6$ the expected accuracy is likely to 60% regardless of humans or machines especially when the sample size is large enough. Richie et. al. [31] show that low IRA is not the ceiling of machine learning performance, by demonstrating that models can score 67% F1 and while humans score 57% under high uncertainty, while acknowledging that high performance is positively correlated with high agreement. If we assume a $p_d = 0.6$ and a sample size of 100, the probability of obtaining an accuracy between 50–60 is around 0.52, while obtaining between 50–70 is 97%, so the fact that models outperform humans — *even if due to chance variation in ground truth* — within this range is not surprising. This is also demonstrated in our empirical results, where models outperform humans under low certainty (despite the models being, in fact, quite weak compared to humans under high certainty), whilst the absolute performance for both models and humans is low under low certainty, as shown in Figure 2. Therefore our argument that under low certainty we might not be able to differentiate between a expert and non-expert holds. With regard to the absolute performance, the probability of obtaining a score of over 80% with at least 100 samples is near zero when $p_d \rightarrow 0.6$, as shown in Table 1 and empirically in Figure 2. Our work fills the gap in interpreting variability in ground truth and providing researchers with a much needed probabilistic paradigm to deal with ground truth uncertainty to measure and compare the performance of automated systems.

6 Conclusion and Recommendations

Large models today can analyze a wide variety of information from X-rays, CT Scans to Ultrasounds [1], with models seemingly capable of achieving expert level performance [34, 26, 37]. While typical metrics superficially might support such findings, a deeper analysis including establishing causation is often required for experiments and corresponding conclusions to be intrinsically valid and minimize the effect of confounders [9, 8, 40, 6].

In this paper, we demonstrated through (a) the probabilistic paradigm of expected accuracy and F1, (b) simulations, and (c) empirically on real world datasets, how absolute performance numbers can be deceptively low for human experts (as well as for any expert AI or algorithmic system) as a

consequence of high variation in ground truth answers. On the flip side, relative metrics comparisons may suggest that a LLM, or any system for that matter, has similar or better than expert performance as seen in areas ranging from radiology [37, 26] to where clinicians prefer AI-generated content over that of their peers [38, 20], but these numbers need not reflect true superior performance. This relative superior performance may be a mirage and tends to be more likely when absolute metrics fail to exceed a rule of thumb threshold of 80%. Specifically, taking the example of binary classification, a random labeller has a $p_r = 0.5$ of selecting the right label, and given a sample size of $N = 30$, the probability of achieving an 80% accuracy or more through chance alone is 2%, suggesting that scores below this level are increasingly susceptible to capability misinterpretation.

To that effect, we make the following recommendations for assessing the quality of evidence presented to support the capability of any system, taking into account the fact that collecting multiple ground truth opinions can be expensive and time consuming.

1. When absolute performance metrics fall below the rule of thumb threshold of 80%, assessing the quality of evidence beyond metrics requires that the results are stratified by probability of the ground truth answer. This probability is typically measured by the agreement on the majority label among multiple ground truth answers collected.
2. The quality of evidence increases with 1) higher performance of the system in high certainty bins 2) sample size of high certainty bins 3) number of ground truth answers collected per item. The report thus must also include the probability of the ground truth answer, ground truth annotation size, sample sizes and positive class ratio of each bin as shown in Table 4.

References

- [1] Rawan AlSaad, Alaa Abd-alrazaq, Sabri Boughorbel, Arfan Ahmed, Max-Antoine Renault, Rafat Damseh, and Javaid Sheikh. Multimodal large language models in health care: Applications, challenges, and future outlook. *J Med Internet Res*, 26:e59505, Sep 2024. ISSN 1438-8871. doi: 10.2196/59505. URL <https://doi.org/10.2196/59505>.
- [2] Xavier Amatriain, Josep M. Pujol, and Nuria Oliver. I like it... i like it not: Evaluating user ratings noise in recommender systems. In Geert-Jan Houben, Gord McCalla, Fabio Pianesi, and Massimo Zancanaro, editors, *User Modeling, Adaptation, and Personalization*, pages 247–258, Berlin, Heidelberg, 2009. Springer Berlin Heidelberg. ISBN 978-3-642-02247-0.
- [3] Jacopo Amidei, Paul Piwek, and Alistair Willis. Agreement is overrated: A plea for correlation to assess human evaluation reliability. In Kees van Deemter, Chenghua Lin, and Hiroya Takamura, editors, *Proceedings of the 12th International Conference on Natural Language Generation*, pages 344–354, Tokyo, Japan, October–November 2019. Association for Computational Linguistics. doi: 10.18653/v1/W19-8642. URL <https://aclanthology.org/W19-8642/>.
- [4] Viraj Bhise, Suja S Rajan, Dean F Sittig, Robert O Morgan, Pooja Chaudhary, and Hardeep Singh. Defining and measuring diagnostic uncertainty in medicine: A systematic review. *J. Gen. Intern. Med.*, 33(1):103–115, January 2018.
- [5] Jacob Cohen. A coefficient of agreement for nominal scales. *Educ. Psychol. Meas.*, 20(1): 37–46, April 1960.
- [6] Irina Degtiar and Sherri Rose. A review of generalizability and transportability. *Annu. Rev. Stat. Appl.*, 10(1):501–524, March 2023.
- [7] Nora Eisemann, Stefan Bunk, Trasias Mukama, Hannah Baltus, Susanne A Elsner, Timo Gomille, Gerold Hecht, Sylvia Heywang-Köbrunner, Regine Rathmann, Katja Siegmann-Luz, Thilo Töllner, Toni Werner Vomweg, Christian Leibig, and Alexander Katalinic. Nationwide real-world implementation of AI for cancer detection in population-based mammography screening. *Nat. Med.*, 31(3):917–924, March 2025.
- [8] Aparna Elangovan, Jiayuan He, and Karin Verspoor. Memorization vs. generalization : Quantifying data leakage in NLP performance evaluation. In Paola Merlo, Jorg Tiedemann, and Reut Tsarfaty, editors, *Proceedings of the 16th Conference of the European Chapter of the Association for Computational Linguistics: Main Volume*, pages 1325–1335, Online, April

2021. Association for Computational Linguistics. doi: 10.18653/v1/2021.eacl-main.113. URL <https://aclanthology.org/2021.eacl-main.113/>.
- [9] Aparna Elangovan, Jiayuan He, Yuan Li, and Karin Verspoor. Principles from clinical research for NLP model generalization. In Kevin Duh, Helena Gomez, and Steven Bethard, editors, *Proceedings of the 2024 Conference of the North American Chapter of the Association for Computational Linguistics: Human Language Technologies (Volume 1: Long Papers)*, pages 2293–2309, Mexico City, Mexico, June 2024. Association for Computational Linguistics. doi: 10.18653/v1/2024.naacl-long.127. URL <https://aclanthology.org/2024.naacl-long.127/>.
- [10] Aparna Elangovan, Lei Xu, Jongwoo Ko, Mahsa Elyasi, Ling Liu, Sravan Babu Bodapati, and Dan Roth. Beyond correlation: The impact of human uncertainty in measuring the effectiveness of automatic evaluation and LLM-as-a-judge, 2025. URL <https://openreview.net/forum?id=E8gYIrbP00>.
- [11] Amos Esty. Navigating the uncertainties of medicine, Jul 2024. URL <https://magazine.hms.harvard.edu/articles/navigating-uncertainties-medicine>.
- [12] David Eubanks. (re) visualizing rater agreement: Beyond single-parameter measures. *Journal of Writing Analytics*, 1, 2017.
- [13] A. Gawande. *Complications: A Surgeon’s Notes on an Imperfect Science*. Henry Holt and Company, 2003. ISBN 9781429972109. URL <https://books.google.com/books?id=8dkuoAz9-WMC>.
- [14] Sandy M. Green, Abelardo Martinez-Rumayor, Shawn A. Gregory, Aaron L. Baggish, Michelle L. O’Donoghue, Jamie A. Green, Kent B. Lewandrowski, and Jr Januzzi, James L. Clinical uncertainty, diagnostic accuracy, and outcomes in emergency department patients presenting with dyspnea. *Archives of Internal Medicine*, 168(7):741–748, 04 2008. ISSN 0003-9926. doi: 10.1001/archinte.168.7.741. URL <https://doi.org/10.1001/archinte.168.7.741>.
- [15] Paul K J Han, Tania D Strout, Caitlin Gutheil, Carl Germann, Brian King, Eirik Ofstad, Pål Gulbrandsen, and Robert Trowbridge. How physicians manage medical uncertainty: A qualitative study and conceptual taxonomy. *Med. Decis. Making*, 41(3):275–291, April 2021.
- [16] Steven Hatch. *Snowball in a blizzard: a physician’s notes on uncertainty in medicine*. Basic Books, 2016.
- [17] Marieka A Helou, Deborah DiazGranados, Michael S Ryan, and John W Cyrus. Uncertainty in decision making in medicine: A scoping review and thematic analysis of conceptual models. *Acad. Med.*, 95(1):157–165, January 2020.
- [18] Jeremy Irvin, Pranav Rajpurkar, Michael Ko, Yifan Yu, Silviana Ciurea-Ilcus, Chris Chute, Henrik Marklund, Behzad Haghgoo, Robyn Ball, Katie Shpanskaya, Jayne Seekins, David A Mong, Safwan S Halabi, Jesse K Sandberg, Ricky Jones, David B Larson, Curtis P Langlotz, Bhavik N Patel, Matthew P Lungren, and Andrew Y Ng. CheXpert: Chest X-Rays, 2019.
- [19] Di Jin, Eileen Pan, Nassim Oufattole, Wei-Hung Weng, Hanyi Fang, and Peter Szolovits. What disease does this patient have? a large-scale open domain question answering dataset from medical exams. *arXiv preprint arXiv:2009.13081*, 2020.
- [20] Eunbeen Jo, Sanghoun Song, Jong-Ho Kim, Subin Lim, Ju Hyeon Kim, Jung-Joon Cha, Young-Min Kim, and Hyung Joon Joo. Assessing GPT-4’s performance in delivering medical advice: Comparative analysis with human experts. *JMIR Med. Educ.*, 10:e51282, July 2024.
- [21] Daniel Kahneman and Amos Tversky. Variants of uncertainty. *Cognition*, 11(2):143–157, 1982.
- [22] Daniel Kahneman, Olivier Sibony, and Cass R. Sunstein. *Noise: a flaw in human judgment*. Little, Brown Spark, New York, first edition edition, 2021. ISBN 978-0-316-45140-6 978-0-316-26665-9. OCLC: on1249942231.
- [23] Kangmoon Kim and Young-Mee Lee. Understanding uncertainty in medicine: concepts and implications in medical education. *Korean J. Med. Educ.*, 30(3):181–188, September 2018.

- [24] NamHyeok Kim and Chanjun Park. Inter-annotator agreement in the wild: Uncovering its emerging roles and considerations in real-world scenarios, 2023.
- [25] Klaus Krippendorff. Reliability in content analysis: Some common misconceptions and recommendations. *Human communication research*, 30(3):411–433, 2004.
- [26] Seowoo Lee, Jiwon Youn, Hyungjin Kim, Mansu Kim, and Soon Ho Yoon. CXR-LLaVA: a multimodal large language model for interpreting chest x-ray images. *Eur. Radiol.*, 35(7): 4374–4386, July 2025.
- [27] Daniel M. Lichtstein. Strategies to deal with uncertainty in medicine. *The American Journal of Medicine*, 136(4):339–340, Apr 2023. ISSN 0002-9343. doi: 10.1016/j.amjmed.2022.12.018. URL <https://doi.org/10.1016/j.amjmed.2022.12.018>.
- [28] Joshua Peterson, Ruairidh Battleday, Thomas Griffiths, and Olga Russakovsky. Human uncertainty makes classification more robust, October 2019. Publisher Copyright: © 2019 IEEE.; 17th IEEE/CVF International Conference on Computer Vision, ICCV 2019 ; Conference date: 27-10-2019 Through 02-11-2019.
- [29] Barbara Plank. The “problem” of human label variation: On ground truth in data, modeling and evaluation. In Yoav Goldberg, Zornitsa Kozareva, and Yue Zhang, editors, *Proceedings of the 2022 Conference on Empirical Methods in Natural Language Processing*, pages 10671–10682, Abu Dhabi, United Arab Emirates, December 2022. Association for Computational Linguistics. doi: 10.18653/v1/2022.emnlp-main.731. URL <https://aclanthology.org/2022.emnlp-main.731/>.
- [30] Justus J Randolph. Free-marginal multirater kappa (multirater k [free]): An alternative to fleiss’ fixed-marginal multirater kappa. *Online submission*, 2005.
- [31] Russell Richie, Sachin Grover, and Fuchiang (Rich) Tsui. Inter-annotator agreement is not the ceiling of machine learning performance: Evidence from a comprehensive set of simulations. In Dina Demner-Fushman, Kevin Bretonnel Cohen, Sophia Ananiadou, and Junichi Tsujii, editors, *Proceedings of the 21st Workshop on Biomedical Language Processing*, pages 275–284, Dublin, Ireland, May 2022. Association for Computational Linguistics. doi: 10.18653/v1/2022.bionlp-1.26. URL <https://aclanthology.org/2022.bionlp-1.26/>.
- [32] Gustavo Saposnik, Donald Redelmeier, Christian C. Ruff, and Philippe N. Tobler. Cognitive biases associated with medical decisions: a systematic review. *BMC Medical Informatics and Decision Making*, 16(1):138, Nov 2016. ISSN 1472-6947. doi: 10.1186/s12911-016-0377-1. URL <https://doi.org/10.1186/s12911-016-0377-1>.
- [33] Karan Singhal, Tao Tu, Juraj Gottweis, Rory Sayres, Ellery Wulczyn, Mohamed Amin, Le Hou, Kevin Clark, Stephen R Pfohl, Heather Cole-Lewis, Darlene Neal, Qazi Mamunur Rashid, Mike Schaekermann, Amy Wang, Dev Dash, Jonathan H Chen, Nigam H Shah, Sami Lachgar, Philip Andrew Mansfield, Sushant Prakash, Bradley Green, Ewa Dominowska, Blaise Agüera Y Arcas, Nenad Tomašev, Yun Liu, Renee Wong, Christopher Semturs, S Sara Mahdavi, Joelle K Barral, Dale R Webster, Greg S Corrado, Yossi Matias, Shekoofeh Azizi, Alan Karthikesalingam, and Vivek Natarajan. Toward expert-level medical question answering with large language models. *Nat. Med.*, 31(3):943–950, March 2025.
- [34] Karan Singhal, Tao Tu, Juraj Gottweis, Rory Sayres, Ellery Wulczyn, Mohamed Amin, Le Hou, Kevin Clark, Stephen R Pfohl, Heather Cole-Lewis, Darlene Neal, Qazi Mamunur Rashid, Mike Schaekermann, Amy Wang, Dev Dash, Jonathan H Chen, Nigam H Shah, Sami Lachgar, Philip Andrew Mansfield, Sushant Prakash, Bradley Green, Ewa Dominowska, Blaise Agüera Y Arcas, Nenad Tomašev, Yun Liu, Renee Wong, Christopher Semturs, S Sara Mahdavi, Joelle K Barral, Dale R Webster, Greg S Corrado, Yossi Matias, Shekoofeh Azizi, Alan Karthikesalingam, and Vivek Natarajan. Toward expert-level medical question answering with large language models. *Nat. Med.*, 31(3):943–950, March 2025.
- [35] David Stutz, Ali Taylan Cemgil, Abhijit Guha Roy, Tatiana Matejovicova, Melih Barsbey, Patricia Strachan, Mike Schaekermann, Jan Freyberg, Rajeev Rikhye, Beverly Freeman, Javier Perez Matos, Umesh Telang, Dale R. Webster, Yuan Liu, Greg S. Corrado, Yossi Matias,

- Pushmeet Kohli, Yun Liu, Arnaud Doucet, and Alan Karthikesalingam. Evaluating medical ai systems in dermatology under uncertain ground truth. *Medical Image Analysis*, 103: 103556, 2025. ISSN 1361-8415. doi: <https://doi.org/10.1016/j.media.2025.103556>. URL <https://www.sciencedirect.com/science/article/pii/S1361841525001033>.
- [36] Debby ten Hove, Terrence D. Jorgensen, and L. Andries van der Ark. On the usefulness of interrater reliability coefficients. In Marie Wiberg, Steven Culpepper, Rianne Janssen, Jorge González, and Dylan Molenaar, editors, *Quantitative Psychology*, pages 67–75, Cham, 2018. Springer International Publishing. ISBN 978-3-319-77249-3.
- [37] Ekin Tiu, Ellie Talius, Pujan Patel, Curtis P. Langlotz, Andrew Y. Ng, and Pranav Rajpurkar. Expert-level detection of pathologies from unannotated chest x-ray images via self-supervised learning. *Nature Biomedical Engineering*, 6(12):1399–1406, Dec 2022. ISSN 2157-846X. doi: [10.1038/s41551-022-00936-9](https://doi.org/10.1038/s41551-022-00936-9). URL <https://doi.org/10.1038/s41551-022-00936-9>.
- [38] Dave Van Veen, Cara Van Uden, Louis Blankemeier, Jean-Benoit Delbrouck, Asad Aali, Christian Bluethgen, Anuj Pareek, Malgorzata Polacin, Eduardo Pontes Reis, Anna Seehofnerová, Nidhi Rohatgi, Poonam Hosamani, William Collins, Neera Ahuja, Curtis P Langlotz, Jason Hom, Sergios Gatidis, John Pauly, and Akshay S Chaudhari. Adapted large language models can outperform medical experts in clinical text summarization. *Nat. Med.*, 30(4):1134–1142, April 2024.
- [39] Yuxia Wang, Shimin Tao, Ning Xie, Hao Yang, Timothy Baldwin, and Karin Verspoor. Collective human opinions in semantic textual similarity. *Transactions of the Association for Computational Linguistics*, 11:997–1013, 08 2023. ISSN 2307-387X. doi: [10.1162/tac1_a_00584](https://doi.org/10.1162/tac1_a_00584). URL https://doi.org/10.1162/tac1_a_00584.
- [40] P M Wortman. Evaluation research: A methodological perspective. *Annu. Rev. Psychol.*, 34(1): 223–260, January 1983.
- [41] Jun S. Liu Xinshu Zhao and Ke Deng. Assumptions behind intercoder reliability indices. *Annals of the International Communication Association*, 36(1):419–480, 2013. doi: [10.1080/23808985.2013.11679142](https://doi.org/10.1080/23808985.2013.11679142). URL <https://doi.org/10.1080/23808985.2013.11679142>.

Appendix A Prompts

The models were prompted as follows “Given the patient’s chest x-ray, answer the following questions: Does this patient have {{condition }}?” with default temperature settings.

Appendix B Simulation details

The simulation was conducted by creating 10 annotations per item with varying p_d , where each annotation was 1 or 0 mimicking binary classification problems. The sample size of the simulation was sampling 500 items per run and controlled for positive class ratio m .

Appendix C Label distribution in CheXpert dataset

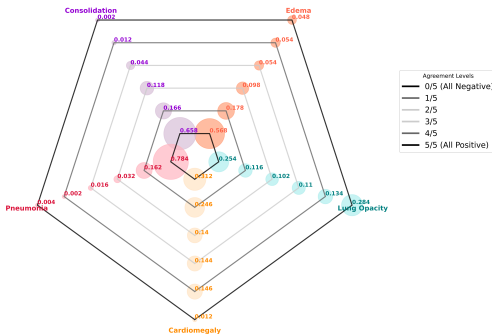


Figure 4: Proportion of samples (CheXpert test set with 500 samples) by agreement level as annotated by 5 radiologists independently. The number of samples with 100% agreement ($p_d = 1.0$) on positive findings drops dramatically to less than 0.01 for 4 of 5 the pathologies. The exception is lung opacity, where the proportion of samples approximately remains the same regardless of agreement levels. Agreement level for all pathologies are in Appendix 5.

Appendix D Performance on other datasets

Dataset	p_d	S	$E(A)$	H'	$\Delta_{EH'}$	M	Δ_{EM}
MNLI M $\langle GT = 5, L=3 \rangle$	0.40	185	0.40	0.42 ± 0.04	-0.019459	nan	NaN
	0.60	1599	0.60	0.60 ± 0.02	0.002251	0.61	-0.010000
	0.80	2457	0.80	0.80 ± 0.01	0.000081	0.78	0.020000
	1.00	5759	1.00	1.00 ± 0.00	0.000000	0.89	0.110000
MNLI MM $\langle GT = 5, L=3 \rangle$	0.40	168	0.40	0.39 ± 0.04	0.009524	nan	NaN
	0.60	1446	0.60	0.61 ± 0.01	-0.007469	0.62	-0.020000
	0.80	2402	0.80	0.80 ± 0.01	0.002331	0.77	0.030000
	1.00	5984	1.00	1.00 ± 0.00	0.000000	0.90	0.100000

Table 5: Expected accuracy (A) vs empirical accuracy. Here M is the existing result on Model Sonnet by Elangovan et al [10]. **GT** is the number of ground truth annotations and L is the number of labels. H' is the performance of another Human. $\Delta_{EM} = E(A) - M$, $\Delta_{EH'} = E(A) - H'$

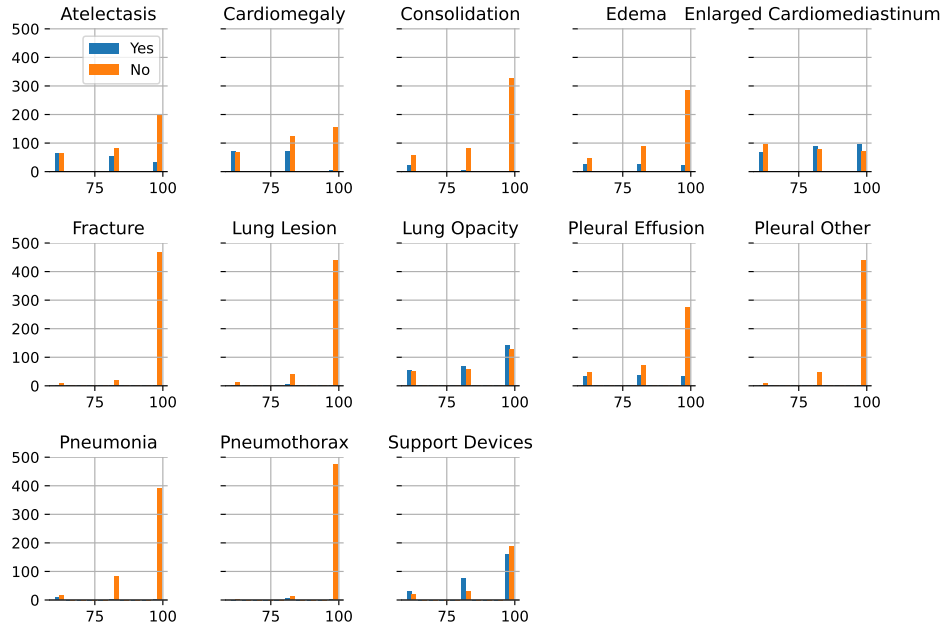


Figure 5: Chest x ray agreement for binary classification across 13 labels. The agreement is across 5 radiologists. The x-axis shows the percentage agreement for the majority label (yes/ no) and the corresponding y-axis indicate the total number of records with that agreement. For instance, for Atelectasis, 100% agreement (5 out of 5 radiologists) is observed for 32 records for a positive finding (yes), while 100% agreement for negative finding for 200 records.

Appendix E Full performance of CheXpert dataset on various model

Pathology	p_d	S	m	F1			Precision			Recall			Accuracy		
				GP	H	Δ	GP	H	Δ	GP	H	Δ	GP	H	Δ
Atelectasis	0.6	130	0.500	0.57	0.66±0.03	0.09	0.53	0.58±0.02	0.05	0.62	0.76±0.10	0.14	0.53	0.60±0.02	0.07
	0.8	140	0.400	0.63	0.70±0.03	0.07	0.57	0.62±0.05	0.05	0.70	0.83±0.11	0.13	0.67	0.73±0.03	0.06
	1.0	230	0.139	0.67	0.74±0.03	0.07	0.54	0.66±0.08	0.12	0.91	0.88±0.13	-0.03	0.88	0.91±0.02	0.03
	All	500	0.306	0.62	0.69±0.02	0.07	0.55	0.61±0.04	0.06	0.71	0.81±0.11	0.10	0.73	0.78±0.02	0.05
Cardio-megaly	0.6	142	0.507	0.67	0.64±0.10	-0.03	0.61	0.71±0.09	0.10	0.75	0.62±0.22	-0.13	0.63	0.66±0.03	0.03
	0.8	196	0.372	0.69	0.71±0.04	0.02	0.59	0.74±0.11	0.15	0.82	0.72±0.15	-0.10	0.72	0.79±0.03	0.07
	1.0	162	0.037	0.35	0.70±0.12	0.35	0.24	0.69±0.17	0.45	0.67	0.78±0.25	0.11	0.91	0.98±0.02	0.07
	All	500	0.302	0.66	0.68±0.07	0.02	0.57	0.72±0.11	0.15	0.78	0.68±0.19	-0.10	0.75	0.81±0.03	0.06
Consolidation	0.6	81	0.272	0.49	0.44±0.07	-0.05	0.40	0.40±0.07	0.00	0.64	0.50±0.12	-0.14	0.64	0.66±0.06	0.02
	0.8	89	0.067	0.36	0.36±0.17	0.00	0.22	0.31±0.25	0.09	1.00	0.61±0.19	-0.39	0.76	0.82±0.11	0.06
	1.0	330	0.003	0.00	0.23±0.21	0.23	0.00	0.14±0.13	0.14	0.00	0.67±0.58	0.67	0.92	0.98±0.01	0.06
	All	500	0.058	0.34	0.39±0.06	0.05	0.23	0.32±0.11	0.09	0.69	0.53±0.11	-0.16	0.85	0.90±0.03	0.05
Edema	0.6	76	0.355	0.56	0.50±0.03	-0.06	0.75	0.48±0.09	-0.27	0.44	0.55±0.13	0.11	0.75	0.60±0.09	-0.15
	0.8	116	0.233	0.44	0.57±0.07	0.13	0.64	0.51±0.10	-0.13	0.33	0.67±0.13	0.34	0.80	0.76±0.07	-0.04
	1.0	308	0.078	0.58	0.70±0.07	0.12	0.79	0.63±0.13	-0.16	0.46	0.79±0.15	0.33	0.95	0.94±0.02	-0.01
	All	500	0.156	0.52	0.58±0.02	0.06	0.73	0.54±0.08	-0.19	0.41	0.67±0.11	0.26	0.88	0.85±0.03	-0.03
Enlarged Cardiome-diastinum	0.6	163	0.417	0.05	0.51±0.06	0.46	0.29	0.65±0.05	0.36	0.03	0.43±0.11	0.40	0.56	0.66±0.02	0.10
	0.8	170	0.529	0.28	0.75±0.04	0.47	0.94	0.94±0.05	0.00	0.17	0.62±0.08	0.45	0.55	0.78±0.02	0.23
	1.0	167	0.569	0.46	0.92±0.03	0.46	1.00	0.99±0.00	-0.01	0.29	0.86±0.05	0.57	0.60	0.91±0.03	0.31
	All	500	0.506	0.30	0.75±0.03	0.45	0.88	0.89±0.04	0.01	0.18	0.66±0.07	0.48	0.57	0.79±0.02	0.22
Fracture	0.6	10	0.200	0.00	0.39±0.35	0.39	0.00	0.50±0.50	0.50	0.00	0.33±0.29	0.33	0.80	0.80±0.10	-0.00
	0.8	21	0.143	0.40	0.32±0.34	-0.08	0.50	0.31±0.34	-0.19	0.33	0.33±0.34	0.00	0.86	0.84±0.07	-0.02
	1.0	469	0.000	0.00	0.00±0.00	0.00	0.00	0.00±0.00	0.00	0.00	0.00±0.00	0.00	0.99	0.99±0.00	0.00
	All	500	0.010	0.14	0.30±0.17	0.16	0.11	0.49±0.46	0.38	0.20	0.33±0.23	0.13	0.98	0.98±0.01	0.00
Lung Lesion	0.6	11	0.000	0.00	nan±nan	NaN	0.00	nan±nan	NaN	0.00	nan±nan	NaN	0.82	nan±nan	NaN
	0.8	47	0.106	0.00	0.47±0.12	0.47	0.00	0.89±0.19	0.89	0.00	0.33±0.12	0.33	0.89	0.92±0.02	0.03
	1.0	442	0.007	0.50	0.74±0.07	0.24	1.00	0.70±0.26	-0.30	0.33	0.89±0.19	0.56	1.00	1.00±0.01	-0.00
	All	500	0.016	0.18	0.60±0.04	0.42	0.33	0.75±0.22	0.42	0.12	0.54±0.14	0.42	0.98	0.99±0.00	0.01
Lung Opacity	0.6	106	0.519	0.57	0.63±0.07	0.06	0.63	0.64±0.01	0.01	0.53	0.62±0.13	0.09	0.59	0.62±0.03	0.03
	0.8	125	0.536	0.83	0.84±0.03	0.01	0.83	0.87±0.05	0.04	0.82	0.82±0.06	-0.00	0.82	0.83±0.03	0.01
	1.0	269	0.528	0.89	0.96±0.01	0.07	0.95	0.95±0.02	-0.00	0.84	0.98±0.02	0.14	0.89	0.96±0.01	0.07
	All	500	0.528	0.81	0.86±0.02	0.05	0.86	0.87±0.03	0.01	0.77	0.86±0.05	0.09	0.81	0.86±0.01	0.05
Pleural Effusion	0.6	83	0.422	0.52	0.61±0.08	0.09	0.44	0.55±0.12	0.11	0.63	0.69±0.03	0.06	0.51	0.62±0.11	0.11
	0.8	110	0.336	0.56	0.78±0.07	0.22	0.46	0.70±0.13	0.24	0.73	0.91±0.07	0.18	0.62	0.82±0.07	0.20
	1.0	307	0.104	0.57	0.83±0.08	0.26	0.44	0.75±0.14	0.31	0.84	0.94±0.05	0.10	0.87	0.96±0.02	0.09
	All	500	0.208	0.55	0.74±0.08	0.19	0.44	0.66±0.13	0.22	0.73	0.85±0.04	0.12	0.75	0.87±0.05	0.12
Pleural Other	0.6	12	0.167	0.00	0.50±0.00	0.50	0.00	0.50±0.00	0.50	0.00	0.50±0.00	0.50	0.83	0.83±0.00	0.00
	0.8	49	0.041	0.00	0.23±0.25	0.23	0.00	0.15±0.17	0.15	0.00	0.50±0.50	0.50	0.96	0.89±0.06	-0.07
	1.0	439	0.000	NaN	0.00±0.00	NaN	NaN	0.00±0.00	NaN	NaN	0.00±0.00	NaN	NaN	0.99±0.01	NaN
	All	500	0.008	0.00	0.26±0.08	0.26	0.00	0.19±0.05	0.19	0.00	0.50±0.25	0.50	0.99	0.98±0.01	-0.01
Pneumonia	0.6	24	0.333	0.57	0.22±0.08	-0.35	0.46	0.50±0.44	0.04	0.75	0.16±0.08	-0.59	0.62	0.60±0.11	-0.02
	0.8	82	0.012	0.12	0.30±0.17	0.18	0.06	0.18±0.13	0.12	1.00	1.00±0.00	0.00	0.82	0.93±0.05	0.11
	1.0	394	0.005	0.08	0.34±0.29	0.26	0.04	0.23±0.23	0.19	0.50	0.67±0.29	0.17	0.94	0.98±0.01	0.04
	All	500	0.022	0.25	0.27±0.13	0.02	0.15	0.26±0.21	0.11	0.73	0.33±0.05	-0.40	0.90	0.95±0.02	0.05
Pneumothorax	0.6	3	0.000	NaN	0.00±0.00	NaN	NaN	0.00±0.00	NaN	NaN	0.00±0.00	NaN	NaN	0.50±0.24	NaN
	0.8	20	0.300	0.29	0.68±0.22	0.39	1.00	0.74±0.07	-0.26	0.17	0.67±0.34	0.50	0.75	0.83±0.08	0.08
	1.0	477	0.006	0.36	0.75±0.25	0.39	0.25	0.87±0.23	0.62	0.67	0.78±0.39	0.11	0.99	1.00±0.00	0.01
	All	500	0.018	0.33	0.66±0.17	0.33	0.33	0.70±0.06	0.37	0.33	0.70±0.34	0.37	0.98	0.99±0.00	0.01
Support Devices	0.6	50	0.580	0.75	0.72±0.04	-0.03	0.60	0.75±0.12	0.15	1.00	0.74±0.20	-0.26	0.62	0.67±0.05	0.05
	0.8	105	0.705	0.86	0.93±0.02	0.07	0.77	0.95±0.04	0.18	0.96	0.92±0.06	-0.04	0.77	0.90±0.02	0.13
	1.0	345	0.458	0.76	0.98±0.00	0.22	0.62	0.99±0.02	0.37	0.96	0.97±0.02	0.01	0.72	0.98±0.00	0.26
	All	500	0.522	0.78	0.93±0.01	0.15	0.66	0.95±0.05	0.29	0.97	0.93±0.05	-0.04	0.72	0.93±0.01	0.21

Table 6: Performance of Gemini Pro 3.0 Preview (GP) model vs. human (H) radiologists, compared against ground truth (majority label across 5 human radiologists). The data is stratified by p_d probability of observed agreement among the 5 radiologists for the majority label. Size (S) is the number of samples corresponding to that p_d , positive class ratio is m . H is the average performance of additional 3 radiologists and the corresponding standard deviation. Humans achieve a peak F1-score of over **0.98** @ $n_A = 1.0$, while the best performance at $n_A = 0.6$ is **0.72** across all pathologies.

Pathology	p_d	S	m	F1			Precision			Recall			Accuracy		
				GP	H	Δ	GP	H	Δ	GP	H	Δ	GP	H	Δ
Atelectasis	60	130	0.500	0.65	0.66±0.03	0.01	0.51	0.58±0.02	0.07	0.91	0.76±0.10	-0.15	0.52	0.60±0.02	0.08
	80	140	0.400	0.62	0.70±0.03	0.08	0.46	0.62±0.05	0.16	0.95	0.83±0.11	-0.12	0.53	0.73±0.03	0.20
	100	230	0.139	0.40	0.74±0.03	0.34	0.25	0.66±0.08	0.41	0.97	0.88±0.13	-0.09	0.60	0.91±0.02	0.31
	All	500	0.306	0.56	0.69±0.02	0.13	0.40	0.61±0.04	0.21	0.93	0.81±0.11	-0.12	0.56	0.78±0.02	0.22
Cardio-megaly	60	142	0.507	0.69	0.64±0.10	-0.05	0.53	0.71±0.09	0.18	0.96	0.62±0.22	-0.34	0.56	0.66±0.03	0.10
	80	196	0.372	0.61	0.71±0.04	0.10	0.44	0.74±0.11	0.30	0.99	0.72±0.15	-0.27	0.53	0.79±0.03	0.26
	100	162	0.037	0.13	0.70±0.12	0.57	0.07	0.69±0.17	0.62	1.00	0.78±0.25	-0.22	0.52	0.98±0.02	0.46
	All	500	0.302	0.56	0.68±0.07	0.12	0.39	0.72±0.11	0.33	0.97	0.68±0.19	-0.29	0.54	0.81±0.03	0.27
Consolidation	60	81	0.272	0.41	0.44±0.07	0.03	0.28	0.40±0.07	0.12	0.82	0.50±0.12	-0.32	0.37	0.66±0.06	0.29
	80	89	0.067	0.14	0.36±0.17	0.22	0.08	0.31±0.25	0.23	0.83	0.61±0.19	-0.22	0.34	0.82±0.11	0.48
	100	330	0.003	0.00	0.23±0.21	0.23	0.00	0.14±0.13	0.14	0.00	0.67±0.58	0.67	0.67	0.98±0.01	0.31
	All	500	0.058	0.17	0.39±0.06	0.22	0.10	0.32±0.11	0.22	0.79	0.53±0.11	-0.26	0.56	0.90±0.03	0.34
Edema	60	76	0.355	0.54	0.50±0.03	-0.04	0.37	0.48±0.09	0.11	1.00	0.55±0.13	-0.45	0.39	0.60±0.09	0.21
	80	116	0.233	0.41	0.57±0.07	0.16	0.26	0.51±0.10	0.25	1.00	0.67±0.13	-0.33	0.33	0.76±0.07	0.43
	100	308	0.078	0.24	0.70±0.07	0.46	0.13	0.63±0.13	0.50	1.00	0.79±0.15	-0.21	0.50	0.94±0.02	0.44
	All	500	0.156	0.36	0.58±0.02	0.22	0.22	0.54±0.08	0.32	1.00	0.67±0.11	-0.33	0.44	0.85±0.03	0.41
Enlarged Cardiomediastinum	60	163	0.417	0.62	0.51±0.06	-0.11	0.48	0.65±0.05	0.17	0.87	0.43±0.11	-0.44	0.56	0.66±0.02	0.10
	80	170	0.529	0.79	0.75±0.04	-0.04	0.68	0.94±0.05	0.26	0.94	0.62±0.08	-0.32	0.74	0.78±0.02	0.04
	100	167	0.569	0.89	0.92±0.03	0.03	0.81	0.99±0.00	0.18	0.99	0.86±0.05	-0.13	0.86	0.91±0.03	0.05
	All	500	0.506	0.77	0.75±0.03	-0.02	0.66	0.89±0.04	0.23	0.94	0.66±0.07	-0.28	0.72	0.79±0.02	0.07
Fracture	60	10	0.200	0.00	0.39±0.35	0.39	0.00	0.50±0.50	0.50	0.00	0.33±0.29	0.33	0.70	0.80±0.10	0.10
	80	21	0.143	0.40	0.32±0.34	-0.08	0.50	0.31±0.34	-0.19	0.33	0.33±0.34	0.00	0.86	0.84±0.07	-0.02
	100	469	0.000	0.00	0.00±0.00	0.00	0.00	0.00±0.00	0.00	0.00	0.00±0.00	0.00	0.92	0.99±0.00	0.07
	All	500	0.010	0.04	0.30±0.17	0.26	0.02	0.49±0.46	0.47	0.20	0.33±0.23	0.13	0.91	0.98±0.01	0.07
Lung Lesion	60	11	0.000	0.00	nan±nan	NaN	0.00	nan±nan	NaN	0.00	nan±nan	NaN	0.91	nan±nan	NaN
	80	47	0.106	0.00	0.47±0.12	0.47	0.00	0.89±0.19	0.89	0.00	0.33±0.12	0.33	0.87	0.92±0.02	0.05
	100	442	0.007	0.00	0.74±0.07	0.74	0.00	0.70±0.26	0.70	0.00	0.89±0.19	0.89	0.98	1.00±0.01	0.02
	All	500	0.016	0.00	0.60±0.04	0.60	0.00	0.75±0.22	0.75	0.00	0.54±0.14	0.54	0.97	0.99±0.00	0.02
Lung Opacity	60	106	0.519	0.69	0.63±0.07	-0.06	0.54	0.64±0.01	0.10	0.96	0.62±0.13	-0.34	0.56	0.62±0.03	0.06
	80	125	0.536	0.73	0.84±0.03	0.11	0.57	0.87±0.05	0.30	1.00	0.82±0.06	-0.18	0.60	0.83±0.03	0.23
	100	269	0.528	0.79	0.96±0.01	0.17	0.66	0.95±0.02	0.29	0.99	0.98±0.02	-0.01	0.73	0.96±0.01	0.23
	All	500	0.528	0.75	0.86±0.02	0.11	0.61	0.87±0.03	0.26	0.99	0.86±0.05	-0.13	0.66	0.86±0.01	0.20
Pleural Effusion	60	83	0.422	0.59	0.61±0.08	0.02	0.42	0.55±0.12	0.13	0.97	0.69±0.03	-0.28	0.42	0.62±0.11	0.20
	80	110	0.336	0.54	0.78±0.07	0.24	0.37	0.70±0.13	0.33	1.00	0.91±0.07	-0.09	0.44	0.82±0.07	0.38
	100	307	0.104	0.28	0.83±0.08	0.55	0.17	0.75±0.14	0.58	1.00	0.94±0.05	-0.06	0.48	0.96±0.02	0.48
	All	500	0.208	0.43	0.74±0.08	0.31	0.28	0.66±0.13	0.38	0.99	0.85±0.04	-0.14	0.46	0.87±0.05	0.41
Pleural Other	60	12	0.167	0.00	0.50±0.00	0.50	0.00	0.50±0.00	0.50	0.00	0.50±0.00	0.50	0.83	0.83±0.00	0.00
	80	49	0.041	0.00	0.23±0.25	0.23	0.00	0.15±0.17	0.15	0.00	0.50±0.50	0.50	0.94	0.89±0.06	-0.05
	100	439	0.000	NaN	0.00±0.00	NaN	NaN	0.00±0.00	NaN	NaN	0.00±0.00	NaN	NaN	0.99±0.01	NaN
	All	500	0.008	0.00	0.26±0.08	0.26	0.00	0.19±0.05	0.19	0.00	0.50±0.25	0.50	0.99	0.98±0.01	-0.01
Pneumonia	60	24	0.333	0.38	0.22±0.08	-0.16	0.28	0.50±0.44	0.22	0.62	0.16±0.08	-0.46	0.33	0.60±0.11	0.27
	80	82	0.012	0.03	0.30±0.17	0.27	0.02	0.18±0.13	0.16	1.00	1.00±0.00	0.00	0.30	0.93±0.05	0.63
	100	394	0.005	0.02	0.34±0.29	0.32	0.01	0.23±0.23	0.22	0.50	0.67±0.29	0.17	0.68	0.98±0.01	0.30
	All	500	0.022	0.07	0.27±0.13	0.20	0.03	0.26±0.21	0.23	0.64	0.33±0.05	-0.31	0.60	0.95±0.02	0.35
Pneumothorax	60	3	0.000	NaN	0.00±0.00	NaN	NaN	0.00±0.00	NaN	NaN	0.00±0.00	NaN	NaN	0.50±0.24	NaN
	80	20	0.300	0.00	0.68±0.22	0.68	0.00	0.74±0.07	0.74	0.00	0.67±0.34	0.67	0.70	0.83±0.08	0.13
	100	477	0.006	0.50	0.75±0.25	0.25	1.00	0.87±0.23	-0.13	0.33	0.78±0.39	0.45	1.00	1.00±0.00	0.00
	All	500	0.018	0.20	0.66±0.17	0.46	1.00	0.70±0.06	-0.30	0.11	0.70±0.34	0.59	0.98	0.99±0.00	0.01
Support Devices	60	50	0.580	0.73	0.72±0.04	-0.01	0.58	0.75±0.12	0.17	1.00	0.74±0.20	-0.26	0.58	0.67±0.05	0.09
	80	105	0.705	0.84	0.93±0.02	0.09	0.74	0.95±0.04	0.21	0.97	0.92±0.06	-0.05	0.74	0.90±0.02	0.16
	100	345	0.458	0.73	0.98±0.00	0.25	0.58	0.99±0.02	0.41	0.97	0.97±0.02	0.00	0.66	0.98±0.00	0.32
	All	500	0.522	0.76	0.93±0.01	0.17	0.62	0.95±0.05	0.33	0.98	0.93±0.05	-0.05	0.67	0.93±0.01	0.26

Table 7: Performance on CheXpert using Gemini 2.5 pro

Pathology	p_d	S	m	F1			Precision			Recall			Accuracy		
				GP	H	Δ	GP	H	Δ	GP	H	Δ	GP	H	Δ
Atelectasis	60	130	0.500	0.49	0.66±0.03	0.17	0.55	0.58±0.02	0.03	0.45	0.76±0.10	0.31	0.54	0.60±0.02	0.06
	80	140	0.400	0.64	0.70±0.03	0.06	0.70	0.62±0.05	-0.08	0.59	0.83±0.11	0.24	0.74	0.73±0.03	-0.01
	100	230	0.139	0.70	0.74±0.03	0.04	0.86	0.66±0.08	-0.20	0.59	0.88±0.13	0.29	0.93	0.91±0.02	-0.02
	All	500	0.306	0.59	0.69±0.02	0.10	0.66	0.61±0.04	-0.05	0.53	0.81±0.11	0.28	0.77	0.78±0.02	0.01
Cardiomegaly	60	142	0.507	0.59	0.64±0.10	0.05	0.56	0.71±0.09	0.15	0.61	0.62±0.22	0.01	0.56	0.66±0.03	0.10
	80	196	0.372	0.61	0.71±0.04	0.10	0.62	0.74±0.11	0.12	0.60	0.72±0.15	0.12	0.71	0.79±0.03	0.08
	100	162	0.037	0.33	0.70±0.12	0.37	0.22	0.69±0.17	0.47	0.67	0.78±0.25	0.11	0.90	0.98±0.02	0.08
	All	500	0.302	0.58	0.68±0.07	0.10	0.55	0.72±0.11	0.17	0.61	0.68±0.19	0.07	0.73	0.81±0.03	0.08
Consolidation	60	81	0.272	0.43	0.44±0.07	0.01	0.28	0.40±0.07	0.12	0.91	0.50±0.12	-0.41	0.35	0.66±0.06	0.31
	80	89	0.067	0.16	0.36±0.17	0.20	0.09	0.31±0.25	0.22	1.00	0.61±0.19	-0.39	0.30	0.82±0.11	0.52
	100	330	0.003	0.00	0.23±0.21	0.23	0.00	0.14±0.13	0.14	0.00	0.67±0.58	0.67	0.75	0.98±0.01	0.23
	All	500	0.058	0.21	0.39±0.06	0.18	0.12	0.32±0.11	0.20	0.90	0.53±0.11	-0.37	0.61	0.90±0.03	0.29
Edema	60	76	0.355	0.48	0.50±0.03	0.02	0.41	0.48±0.09	0.07	0.59	0.55±0.13	-0.04	0.55	0.60±0.09	0.05
	80	116	0.233	0.64	0.57±0.07	-0.07	0.54	0.51±0.10	-0.03	0.78	0.67±0.13	-0.11	0.79	0.76±0.07	-0.03
	100	308	0.078	0.63	0.70±0.07	0.07	0.51	0.63±0.13	0.12	0.83	0.79±0.15	-0.04	0.93	0.94±0.02	0.01
	All	500	0.156	0.58	0.58±0.02	0.00	0.49	0.54±0.08	0.05	0.73	0.67±0.11	-0.06	0.84	0.85±0.03	0.01
Enlarged Cardiomediastinum	60	163	0.417	0.44	0.51±0.06	0.07	0.56	0.65±0.05	0.09	0.37	0.43±0.11	0.06	0.61	0.66±0.02	0.05
	80	170	0.529	0.66	0.75±0.04	0.09	0.89	0.94±0.05	0.05	0.52	0.62±0.08	0.10	0.71	0.78±0.02	0.07
	100	167	0.569	0.84	0.92±0.03	0.08	0.99	0.99±0.00	-0.00	0.73	0.86±0.05	0.13	0.84	0.91±0.03	0.07
	All	500	0.506	0.67	0.75±0.03	0.08	0.84	0.89±0.04	0.05	0.56	0.66±0.07	0.10	0.72	0.79±0.02	0.07
Fracture	60	10	0.200	0.00	0.39±0.35	0.39	0.00	0.50±0.50	0.50	0.00	0.33±0.29	0.33	0.80	0.80±0.10	-0.00
	80	21	0.143	0.40	0.32±0.34	-0.08	0.50	0.31±0.34	-0.19	0.33	0.33±0.34	0.00	0.86	0.84±0.07	-0.02
	100	469	0.000	0.00	0.00±0.00	0.00	0.00	0.00±0.00	0.00	0.00	0.00±0.00	0.00	1.00	0.99±0.00	-0.01
	All	500	0.010	0.25	0.30±0.17	0.05	0.33	0.49±0.46	0.16	0.20	0.33±0.23	0.13	0.99	0.98±0.01	-0.01
Lung Lesion	80	47	0.106	0.00	0.47±0.12	0.47	0.00	0.89±0.19	0.89	0.00	0.33±0.12	0.33	0.89	0.92±0.02	0.03
	100	442	0.007	0.00	0.74±0.07	0.74	0.00	0.70±0.26	0.70	0.00	0.89±0.19	0.89	0.99	1.00±0.01	0.01
	All	500	0.016	0.00	0.60±0.04	0.60	0.00	0.75±0.22	0.75	0.00	0.54±0.14	0.54	0.98	0.99±0.00	0.01
Lung Opacity	60	106	0.519	0.66	0.63±0.07	-0.03	0.56	0.64±0.01	0.08	0.80	0.62±0.13	-0.18	0.58	0.62±0.03	0.04
	80	125	0.536	0.82	0.84±0.03	0.02	0.75	0.87±0.05	0.12	0.91	0.82±0.06	-0.09	0.79	0.83±0.03	0.04
	100	269	0.528	0.90	0.96±0.01	0.06	0.86	0.95±0.02	0.09	0.95	0.98±0.02	0.03	0.89	0.96±0.01	0.07
	All	500	0.528	0.83	0.86±0.02	0.03	0.76	0.87±0.03	0.11	0.91	0.86±0.05	-0.05	0.80	0.86±0.01	0.06
Pleural Effusion	60	83	0.422	0.51	0.61±0.08	0.10	0.41	0.55±0.12	0.14	0.69	0.69±0.03	0.00	0.45	0.62±0.11	0.17
	80	110	0.336	0.63	0.78±0.07	0.15	0.49	0.70±0.13	0.21	0.86	0.91±0.07	0.05	0.65	0.82±0.07	0.17
	100	307	0.104	0.55	0.83±0.08	0.28	0.40	0.75±0.14	0.35	0.84	0.94±0.05	0.10	0.85	0.96±0.02	0.11
	All	500	0.208	0.56	0.74±0.08	0.18	0.43	0.66±0.13	0.23	0.80	0.85±0.04	0.05	0.74	0.87±0.05	0.13
Pleural Other	60	12	0.167	0.00	0.50±0.00	0.50	0.00	0.50±0.00	0.50	0.00	0.50±0.00	0.50	0.83	0.83±0.00	0.00
	80	49	0.041	0.00	0.23±0.25	0.23	0.00	0.15±0.17	0.15	0.00	0.50±0.50	0.50	0.96	0.89±0.06	-0.07
	100	439	0.000	0.00	0.00±0.00	0.00	0.00	0.00±0.00	0.00	0.00	0.00±0.00	0.00	1.00	0.99±0.01	-0.01
	All	500	0.008	0.00	0.26±0.08	0.26	0.00	0.19±0.05	0.19	0.00	0.50±0.25	0.50	0.99	0.98±0.01	-0.01
Pneumonia	60	24	0.333	0.43	0.22±0.08	-0.21	0.30	0.50±0.44	0.20	0.75	0.16±0.08	-0.59	0.33	0.60±0.11	0.27
	80	82	0.012	0.03	0.30±0.17	0.27	0.02	0.18±0.13	0.16	1.00	1.00±0.00	0.00	0.26	0.93±0.05	0.67
	100	394	0.005	0.02	0.34±0.29	0.32	0.01	0.23±0.23	0.22	0.50	0.67±0.29	0.17	0.67	0.98±0.01	0.31
	All	500	0.022	0.07	0.27±0.13	0.20	0.04	0.26±0.21	0.22	0.73	0.33±0.05	-0.40	0.59	0.95±0.02	0.36
Pneumothorax	60	3	0.000	NaN	0.00±0.00	NaN	NaN	0.00±0.00	NaN	NaN	0.00±0.00	NaN	NaN	0.50±0.24	NaN
	80	20	0.300	0.00	0.68±0.22	0.68	0.00	0.74±0.07	0.74	0.00	0.67±0.34	0.67	0.70	0.83±0.08	0.13
	100	477	0.006	0.00	0.75±0.25	0.75	0.00	0.87±0.23	0.87	0.00	0.78±0.39	0.78	0.99	1.00±0.00	0.01
	All	500	0.018	0.00	0.66±0.17	0.66	0.00	0.70±0.06	0.70	0.00	0.70±0.34	0.70	0.98	0.99±0.00	0.01
Support Devices	60	50	0.580	0.74	0.72±0.04	-0.02	0.59	0.75±0.12	0.16	1.00	0.74±0.20	-0.26	0.60	0.67±0.05	0.07
	80	105	0.705	0.85	0.93±0.02	0.08	0.76	0.95±0.04	0.19	0.96	0.92±0.06	-0.04	0.76	0.90±0.02	0.14
	100	345	0.458	0.76	0.98±0.00	0.22	0.63	0.99±0.02	0.36	0.96	0.97±0.02	0.01	0.72	0.98±0.00	0.26
	All	500	0.522	0.78	0.93±0.01	0.15	0.66	0.95±0.05	0.29	0.96	0.93±0.05	-0.03	0.72	0.93±0.01	0.21

Table 8: Performance of GPT 5.1 on CheXpert